LIFE SCIENCE REVIEW

Original Research Article Journal homepage: https://lsr.crcjournals.org/

p-ISSN 3117-3535
e-ISSN 3117-3543

Check for updates

In vitro Evaluation, Green Synthesis Characterization and Molecular Docking for Medicinal Target Prediction of Gumbo Limbo *(Bursera simaruba)*

Adewumi F. A.*[1], Oseni M. O.[2], Ndubueze D. I.[3], Airaodion A. I.[4] and Oseni O. A.[5]

[1]*Department of Medical Laboratory Science, Faculty of Basic Medical Sciences, College of Medicine, Ekiti State University, Ado-Ekiti, Nigeria*
[2]*Department of Chemistry, Faculty of Science, Federal University, Oye- Ekiti, Nigeria*
[3]*Department of Science Laboratory Technology, Faculty of Science, Ekiti State University, Ado-Ekiti, Nigeria*
[4]*Department of Biochemistry, Faculty of Natural and Applied Sciences, Lead City University, Ibadan, Oyo State, Nigeria*
[5]*Department of Medical Biochemistry, Faculty of Basic Medical Sciences, College of Medicine, Ekiti State University, Ado- Ekiti, Nigeria*

Received 10 January 2026 | Revised 05 February 2026 | Accepted 07 March 2026 | Available Online 02 April 2026

*Corresponding Author: **Adewumi F. A** | Email Address: **funmilayo.adewumi@eksu.edu.ng**

Citation: Adewumi F. A., Oseni M. O., Ndubueze D. I., Airaodion A. I. and Oseni O. A. (2026). *In vitro* Evaluation, Green Synthesis Characterization and Molecular Docking for Medicinal Target Prediction of Gumbo Limbo *(Bursera simaruba)*. ***Life Science Review***. **DOI: https://doi.org/10.51470/LSR.2026.10.01.77**

Abstract

Background: *Bursera simaruba (commonly known as gumbo limbo) is a well-recognized medicinal plant traditionally employed in the treatment of inflammatory and metabolic conditions. Despite its widespread ethnomedicinal use, there is still a lack of comprehensive scientific evidence that combines phytochemical characterization, eco-friendly nanoparticle synthesis, antimicrobial assessment, and molecular docking approaches for identifying its therapeutic targets.*

Objective: *This study was designed to investigate the in vitro antioxidant and antimicrobial activities of the aqueous leaf extract of Bursera simaruba. It also sought to synthesize and characterize plant-mediated metallic nanoparticles (silver, copper, and zinc oxide) and to explore potential therapeutic targets through molecular docking analysis.*

Materials and Methods: *Bursera simaruba fresh leaves were gathered, verified, and extracted with distilled water. In addition to quantitative antioxidant tests such as DPPH radical scavenging, ferric reducing antioxidant power (FRAP), nitric oxide inhibition, total phenolic content (TPC), total flavonoid content (TFC), and vitamin C determination, preliminary phytochemical screening was carried out. Proximate composition, mineral content, and antinutritional components were assessed using standard analytical techniques. The plant extract was used as a reducing and stabilising agent in the green synthesis of silver (AgNPs), copper (CuNPs), and zinc oxide nanoparticles (ZnONPs). Fourier Transform Infrared (FTIR) analysis and UV-visible spectroscopy were used to characterise the produced nanoparticles. A few bacterial and fungal isolates were used to investigate the antimicrobial activity. Additionally, in silico ADME profiling and molecular docking experiments were carried out against dipeptidyl peptidase-4 (DPP4).*

Results: *The findings revealed that the leaf extract possesses notable nutritional value, with relatively high carbohydrate (33.65%) and protein (17.11%) contents, along with appreciable mineral levels. Phytochemical analysis confirmed the presence of bioactive constituents such as saponins, phenols, and alkaloids. Quantitative assays indicated elevated flavonoid (82.86 mg AAE/g) and phenolic (57.00 mg GAE/g) concentrations, accompanied by strong antioxidant performance (nitric oxide inhibition of 75.00%, FRAP value of 66.01%, and DPPH activity of 57.00%). Successful nanoparticle formation was verified through characteristic surface plasmon resonance peaks and FTIR-identified functional groups. The synthesized nanoparticles demonstrated superior antibacterial and antifungal effects compared to the crude extract, with copper and silver nanoparticles showing the highest inhibitory activity. Molecular docking analysis revealed strong binding affinities toward DPP4, particularly for compounds such as 4-dimethylamino-3,5-dinitrobenzoic acid (−6.8 kcal/mol) and squalene (−6.2 kcal/mol), indicating possible antidiabetic potential. ADME predictions further suggested that several of the identified compounds possess favorable pharmacokinetic profiles.*

Conclusion: *Bursera simaruba possesses significant antioxidant and antimicrobial properties and serves as an effective bio-reducing agent for green synthesis of metallic nanoparticles. Molecular docking findings provide mechanistic insight into its potential antidiabetic activity via DPP4 inhibition. These findings scientifically support its ethnomedicinal relevance and highlight its promise for pharmaceutical and nanomedicine applications.*

Keywords: *Bursera simaruba; green synthesis; nanoparticles; antioxidant activity; molecular docking; DPP4 inhibition; phytochemicals.*

INTRODUCTION

Medicinal plants continue to play a central role in the search for biologically active compounds for therapeutic use and drug development. Despite advances in synthetic chemistry and high-throughput screening technologies, a significant proportion of contemporary pharmaceuticals are either directly obtained from plant sources or designed based on the structural framework of plant-derived secondary metabolites. Nearly 80% of people worldwide rely, to some degree, on traditional medicine for basic healthcare, according to the World Health Organization [1]. This is especially true in low- and middle-income nations where plant-based therapies are still both economically and culturally relevant. This continued reliance, alongside the increasing challenges of antimicrobial resistance, chronic inflammatory diseases, cancer prevalence, and emerging viral infections, has strengthened the need to identify and validate new phytochemicals with therapeutic relevance.

One plant that has attracted attention in ethnomedicine is *Bursera simaruba* (L.) Sarg., commonly referred to as Gumbo Limbo. It is widely used across Central America, the Caribbean, and some tropical regions of Africa. As a member of the Burseraceae family, it belongs to a group of resin-producing plants known for their richness in terpenoids, flavonoids, and phenolic constituents. Traditionally, *B. simaruba* has been utilized in the treatment of a wide range of conditions, including inflammation, fever, gastrointestinal disturbances, infections, wounds, and various skin disorders. Ethnobotanical reports highlight the use of different plant parts such as the bark, leaves, and resin, often prepared as decoctions or topical applications [2]. These longstanding uses point toward the presence of active phytochemicals that merit detailed scientific investigation.

Studies exploring the phytochemical profile of *B. simaruba* and related species have identified several important classes of compounds, including triterpenoids, lignans, flavonoids, tannins, and essential oils. Many of these metabolites have demonstrated notable antioxidant, antimicrobial, anti-inflammatory, and cytotoxic activities. In particular, terpenoids derived from members of the Burseraceae family have shown potential in modulating key biological pathways, such as NF-κB signaling and apoptosis, which are relevant in inflammation and cancer. Despite these promising findings, there is still a need for more comprehensive in vitro studies, especially those that integrate molecular target prediction, to better understand their mechanisms of action.

At the same time, nanotechnology has introduced new possibilities in biomedical research, particularly in enhancing the delivery and effectiveness of bioactive compounds. The use of plant extracts in the green synthesis of nanoparticles has emerged as a widely accepted approach due to its sustainability and eco-friendly nature compared to traditional methods. In this process, bioactive constituents found in plants, including polyphenols, flavonoids, and various sugars, play a dual role by facilitating the reduction of metal ions and stabilizing the nanoparticles formed. Compared to traditional chemical methods, this strategy tends to produce nanoparticles with better biocompatibility and lower toxicity [3]. Notably, nanoparticles such as silver, zinc oxide, and gold synthesized through plant-mediated processes have demonstrated improved antimicrobial, antioxidant, anticancer, and anti-inflammatory effects, often due to synergistic interactions between the metal core and the phytochemical coating.

To fully understand and optimize these nanoparticles, proper characterization is essential. A range of analytical techniques is typically employed, alongside a range of characterization techniques such as UV–Visible spectroscopy, Fourier-transform infrared spectroscopy (FTIR), X-ray diffraction (XRD), scanning electron microscopy (SEM), transmission electron microscopy (TEM), and dynamic light scattering (DLS). These methods help confirm nanoparticle formation and provide detailed information about size, structure, surface properties, and stability. Thorough physicochemical characterization not only ensures consistency and reproducibility but also supports accurate evaluation of biological activity, ultimately enhancing the potential for real-world biomedical applications [4].

Beyond experimental validation, computational approaches such as molecular docking have revolutionized early-stage drug discovery by enabling prediction of ligand–protein interactions at the molecular level. Molecular docking provides insights into binding affinity, interaction energy, hydrogen bonding patterns, and active site compatibility between phytochemicals and therapeutic targets. This approach accelerates medicinal target prediction, reduces experimental cost, and guides rational drug development strategies. Recent studies have successfully integrated phytochemical screening with docking simulations to identify potential inhibitors of key targets involved in inflammation (COX-2), cancer (EGFR, Bcl-2), microbial infections (DNA gyrase), and metabolic disorders (α-amylase, DPP-4) [5].

Importantly, combining *in vitro* bioassays with molecular docking enhances the robustness of pharmacological investigations. While *in vitro* assays provide empirical evidence of biological activity, such as antioxidant scavenging capacity, antimicrobial inhibition zones,

cytotoxicity profiles, or enzyme inhibition, molecular docking offers mechanistic explanations at the atomic level. This integrative strategy bridges the gap between ethnomedicine and evidence-based pharmacology.

Despite the documented ethnomedicinal use of *Bursera simaruba*, there remains limited comprehensive research integrating green synthesis of nanoparticles, detailed physicochemical characterization, *in vitro* biological evaluation, and molecular docking-based medicinal target prediction. Most existing studies focus on isolated pharmacological aspects without correlating phytochemical composition to specific molecular targets. Furthermore, given the global urgency to discover novel antimicrobial and anti-inflammatory agents in the era of rising resistance and chronic disease prevalence, systematic evaluation of traditionally valued plants such as Gumbo Limbo is both timely and scientifically justified.

Therefore, this study is designed to investigate the *in vitro* biological potential of *Bursera simaruba*, employ green synthesis approaches for nanoparticle fabrication using its extract, characterize the synthesized nanomaterials using advanced analytical techniques, and utilize molecular docking tools to predict plausible medicinal targets. By integrating phytochemistry, nanotechnology, experimental pharmacology, and computational modelling, this research seeks to provide a multidimensional understanding of the therapeutic potential of Gumbo Limbo and contribute to the expanding field of plant-based nanomedicine and rational drug discovery.

MATERIALS AND METHODS

Plant Identification Authentication

Fresh leaves of *Bursera simaruba* (commonly known as Gumbo limbo) were harvested on March 10, 2025, from Ado-Ekiti in Ekiti State, Nigeria. Botanical identification and authentication were carried out at the herbarium unit of the Department of Plant Science, Faculty of Science, Ekiti State University, Ado-Ekiti. Voucher specimens were prepared and deposited with assigned accession numbers for reference. The plant was further verified by Mr. Omotayo, the Chief Technologist at the facility. Subsequent procedures involving sample preparation, biochemical and antimicrobial evaluation, nanoparticle characterization, and molecular docking for therapeutic target prediction were carefully designed to preserve the integrity and bioactivity of the aqueous leaf extract.

Preparation and Extraction of Plant Material

Fresh leaves of *Bursera simaruba* were carefully harvested and rinsed thoroughly under running tap water to remove adhering dirt, debris, and potential microbial contaminants. The washed leaves were then spread out and allowed to dry in the shade for several days. This approach was deliberately chosen to preserve heat- and light-sensitive phytochemicals, particularly flavonoids and polyphenols, which are prone to degradation when exposed to direct sunlight.

Once completely dried, the leaves were ground into a fine powder using an appropriate milling device.

To enable effective extraction of bioactive components, a weighed quantity (20 g) of the powdered material was submerged in 100 mL of distilled water and permitted to stand overnight with sporadic stirring. Whatman filter paper was then used to filter the mixture, and the resulting clear filtrate was gathered and kept for use in green synthesis, phytochemical analysis, and antioxidant assessment.

Phytochemical Screening (Fresh Extract)

The aqueous extract was subjected to qualitative phytochemical investigations to identify major secondary metabolites, including flavonoids, alkaloids, saponins, phenolics, and steroidal compounds. These analyses were performed using established standard procedures as outlined by Ogbuagu et al. [6].

Determination of DPPH Free Radical Scavenging Activity

Using a slightly modified procedure outlined by Airaodion et al. [7], the DPPH (2,2-diphenyl-1-picrylhydrazyl) radical scavenging experiment was used to evaluate the extract's antioxidant activity. This process involved transferring 1.0 mL of the extract into different test tubes at concentrations of 20, 40, and 80 mg/mL. Each tube received an equivalent volume (1.0 mL) of 0.1 mM methanolic DPPH solution. To ensure that the extract and the DPPH radicals had enough time to interact, the reaction mixtures were thoroughly mixed and allowed to sit at room temperature in the dark for half an hour.

A spectrophotometer was used to assess each sample's absorbance at 516 nm after incubation. The extract's capacity to scavenge radicals was demonstrated by a drop in absorbance when compared to the control. The extract was substituted with distilled water for the control. Next, the conventional formula was used to determine the % inhibition of DPPH radicals:

$$\% \text{ DPPH radical scavenging ability} = 1 - \frac{\text{Absorbance of Sample}}{\text{Absorbance of Control}} \text{ x } 100$$

Determination of Ferric Reducing Antioxidant Power

A slightly modified version of the technique described by Airaodion et al. [8] was used to evaluate the extract's ferric-reducing ability. This technique is predicated on the idea that when excess ferricyanide is present, antioxidants can convert ferric ions (Fe^{3+}) to ferrous ions (Fe^{2+}). Briefly, 1.0 mL of 200 mM sodium phosphate buffer (pH 6.6) and 1.0 mL of 1% potassium ferricyanide solution were combined with different quantities of the methanolic extract (10–50 µg/mL). To enable the process, the resultant mixtures were incubated for 20 minutes at 50 °C. Following incubation, the solutions were cooled before 1.0 mL of 10% trichloroacetic acid (TCA) was added. After that, the samples were centrifuged for ten minutes at 2000 rpm to produce a clear supernatant.

After that, 1.0 mL of the supernatant was moved and mixed with 0.25 mL of a 0.1% ferric chloride solution and 1.0 mL of distilled water.

The control sample had all of the ingredients except potassium ferricyanide, and the blank was distilled water. A spectrophotometer was used to test each sample's absorbance at 700 nm. Higher ferric-reducing antioxidant activity in this experiment is indicated by lower absorbance readings. The following formula was then used to get the % ferric-reducing antioxidant power (FRAP):

$$\text{FRAP (\%)} = \frac{\text{Abs control} - \text{Abs sample}}{\text{Abs control}} \times 100$$

Determination of Total Phenolic Content

According to Airaodion and Onabanjo [9], the Folin-Ciocalteu method was used to measure the total phenolic content. This process involved reacting 0.2 mL of the extract with 2.0 mL of a 7.5% sodium carbonate solution and 1.5 mL of 10% Folin-Ciocalteu reagent. To enable colour development, the mixture was incubated for 40 minutes at 45°C. Next, absorbance was measured at 700 nm.

Milligrams of gallic acid equivalents per gram of dry extract (mg GAE/g) were used to express the phenolic content. A gallic acid calibration curve represented by the following equation was used to accomplish quantification:

$$Y = 0.005x + 0.464 \ (R^2 = 0.961).$$

Determination of Total Flavonoid Content

A colorimetric technique outlined by Esonu et al. [10] was used to determine the total flavonoid content. First, 0.2 mL of the extract and 0.3 mL of 5% sodium nitrite were combined. 0.6 mL of 10% aluminium chloride was added after five minutes. After six minutes, 2.1 mL of distilled water and 2.0 mL of 1 M sodium hydroxide were added to the mixture. After fully mixing the solution, absorbance was measured at 510 nm in comparison to a reagent blank.

Gallic acid equivalents (mg GAE/g of dry extract) were used to express the flavonoid content. Under the same circumstances, a standard gallic acid solution (0.5 mg/mL in methanol) was utilised for calibration. Every analysis was carried out twice. The standard curve equation used was: $Y = 0.005x + 0.464$ ($R^2 = 0.961$).

Estimation of Vitamin C

The determination of ascorbic acid was carried out following the method outlined by Airaodion et al. [11]. Briefly, 0.5 mL and 1.0 mL portions of the filtered sample were transferred into separate volumetric flasks. Bromine water was then carefully added dropwise until a stable coloration persisted, indicating that ascorbic acid had been fully oxidized to dehydroascorbic acid. Any excess bromine present was subsequently neutralized with a few drops of 10% thiourea solution, yielding a clear mixture.

Following this, 0.5 mL of 2,4-dinitrophenylhydrazine (DNPH) reagent (prepared as 2% in 9N H_2SO_4) was introduced and mixed thoroughly. The final volume of the reaction mixture was adjusted to 2 mL using 10% acetic acid. Standard solutions of ascorbic acid (2 mg/mL), ranging from 0.2 to 1.0 mL, were processed under identical conditions.

Absorbance readings were taken at 520 nm, and the vitamin C concentration was determined using a calibration curve generated through linear regression. The results were expressed in milligrams per gram (mg/g) of the sample.

Green Synthesis of Nanoparticles

Nanoparticles were synthesized using the aqueous extract of *Bursera simaruba* in accordance with the procedure described by Adewumi et al. [12].

Antimicrobial Analysis

The antimicrobial properties of the extract were assessed against selected pathogenic microorganisms using standard laboratory techniques. The agar well diffusion method was applied for bacterial isolates, while antifungal activity was evaluated using the mycelial growth inhibition assay, as previously described [13]. The test organisms included *Escherichia coli*, *Streptococcus mutans*, *Salmonella typhi*, *Staphylococcus aureus*, *Klebsiella pneumoniae*, *Macrophomina phaseolina*, and *Alternaria alternata*.

RESULTS

The proximate composition of *Bursera simaruba* leaf revealed that carbohydrates constituted the highest proportion (33.65 ± 0.07%), followed by crude protein (17.11 ± 0.01%), ash (17.07 ± 0.10%), crude fat (15.08 ± 0.11%), crude fibre (10.82 ± 0.10%), and moisture content (6.27 ± 0.05%) as presented in Table 1. Antinutrient analysis showed relatively low oxalate (1.61 ± 0.02 mg/100 g) and tannin (4.14 ± 0.01 mg/100 g) levels, moderate phytate content (13.14 ± 0.06 mg/100 g), and a trypsin inhibitor value of 42.00 ± 1.14% (Table 2).

Mineral profiling indicated potassium (5.25 ± 0.01 mg/100 g) as the most abundant macroelement, followed by calcium (3.91 ± 0.01 mg/100 g), sodium (2.85 ± 0.01 mg/100 g), and magnesium (1.99 ± 0.01 mg/100 g). Trace elements detected included iron (2.19 ± 0.00 ppm), copper (0.49 ± 0.01 ppm), manganese (0.43 ± 0.00 ppm), chromium (0.11 ± 0.00 ppm), and lead (0.10 ± 0.00 ppm) (Table 3).

Qualitative phytochemical screening showed strong presence of saponins (++++) and mild presence of phenolics (+) and alkaloids (+), while anthraquinones, terpenoids, Keller-Killani, and Liebermann's tests were negative (Table 4). Quantitative antioxidant constituents revealed high flavonoid content (82.86 ± 0.02 mg AAE/g), phenolic content (57.00 ± 0.03 mg GAE/g), and vitamin C (1.97 ± 0.02 mg/g) (Table 5), with calibration curves illustrated in Figures 2, 3, and 4. *In vitro* antioxidant assays demonstrated nitric oxide scavenging activity as the highest (75.00 ± 0.02%), followed by FRAP (66.01 ± 0.01%), DPPH (57.00 ± 0.02%), and hydrogen peroxide scavenging (40.00 ± 0.03%) (Table 6).

Antibacterial evaluation showed that the crude extract produced inhibition zones ranging from 2.00–4.00 mm, while silver (AgNP), zinc (ZnNP), and copper (CuNP) nanoparticles exhibited enhanced activity. CuNP showed the highest inhibition against *Streptococcus mutans* (8.50 mm) and *Salmonella typhi* (8.00 mm), while AgNP recorded 8.00 mm

against both *Staphylococcus aureus* and *Klebsiella pneumoniae* (Table 7).

Antifungal activity demonstrated moderate inhibition by the crude extract (60.37% against *Microphomina phaseolina* and 56.32% against *Alternaria alternata*), while nanoparticle formulations showed higher mycelial growth inhibition, particularly AgNP (72.63%) and ZnNP (71.58%) against *M. phaseolina* (Table 8). Nanoparticle synthesis and characterization were confirmed by UV–Visible spectroscopy (Figure 1) and FTIR analyses of the extract and synthesized nanoparticles (Figures 5–8).

Ligand identification of major phytochemicals is presented in Table 9, while predicted ADME properties are summarized in Table 10, showing generally high gastrointestinal absorption for most compounds. Molecular docking analysis against DPP4 revealed binding affinities ranging from −4.3 to −6.8 kcal/mol, with 4-dimethylamino-3,5-dinitrobenzoic acid (−6.8 kcal/mol), benzenepropanoic acid derivative (−6.4 kcal/mol), and squalene (−6.2 kcal/mol) showing the strongest interactions (Table 11). Predicted molecular targets of selected phytochemicals are presented in Table 12.

Target gene network analyses, including transcription factor enrichment (Figure 9a), protein–protein interaction expansion (Figure 9b), kinase enrichment analysis (Figure 9c), and expression-to-kinase network (Figure 9d), further illustrated the molecular interaction landscape. Detailed 2D binding interactions of selected ligands with DPP4 are shown in Figures 10a–10e.

Table 1: Proximate Composition of Bursera simaruba leaf

Parameters	Moisture Content	Ash	Crude fat	Crude Fibre	Crude protein	CHO
Value	6.27±0.05	17.07±0.10	15.08±0.11	10.82±0.10	17.11±0.01	33.65±0.07

Table 2: Antinutrient Composition of Bursera simaruba leaf

Parameters	Oxalate (mg/100g)	Phytate (mg/100g)	Tannin (mg/100g)	Trypsin Inhibitor (%)
Values	1.61±0.02	13.14±0.06	4.14±0.01	42.00±1.14

Table 3: Mineral Composition of Bursera simaruba leaf

K (mg/100)	Na (mg/100)	Ca (mg/100)	Mg (mg/100)	Cu (Ppm)	Fe (Ppm)	Mn (Ppm)	Cr (Ppm)	Pb (Ppm)
5.25±0.01	2.85±0.01	3.91±0.01	1.99±0.01	0.49±0.01	2.19±0.00	0.43±0.00	0.11±0.00	0.10±0.00

Table 4: Phytochemical screening of the Aqueous plant extracts

Parameters	Value
Saponin Test	++++
Phenolic Test	+
Wagner's Test	+
Anthraquinone Test	-
Terpenoid Test	-
Keller-killani Test	-
Lieberman's Test	-

Table 5: Antioxidant potentials of aqueous plant's extracts of Gumbo limbo (Bursera simaruba) leaf

Parameters	Flavonoid Content (mg AAE/g)	Phenolic Content (mg GAE/g)	Vitamin C Content
Values	82.86±0.02	57.00±0.03	1.97±0.02

Table 6: % Antioxidant potentials of aqueous plant extracts of Gumbo limbo (Bursera simaruba) leaf

Parameters	DPPH	H_2O_2	NO	FRAP
Values	57.00±0.02	40.00±0.03	75.00±0.02	66.01±0.01

Table 7: Antibacterial activity of Aqueous extract and the Nanoparticle of Gumbo limbo (Bursera simaruba) leaf on some selected bacteria

Sample	*E. coli*	*Streptococcus mutant*	*Salmonella typhi*	*Staphylococcus aureus*	*Klebsiella pneumoniae*
	Zone inhibition in mm				
Gumbo limbo extract	**3.50**	**2.00**	**4.00**	**3.50**	**3.50**
AgNP	**5.20**	**3.40**	**7.50**	**8.00**	**8.00**
ZnNP	**4.80**	**3.50**	**6.00**	**4.00**	**6.00**
CuNP	**6.50**	**8.50**	**8.00**	**3.80**	**5.00**

Table 8: Antifungal activity of Aqueous extract and the Nanoparticle of Gumbo limbo (Bursera simaruba) leaf on some selected bacteria

Samples	*Microphomina phaseolina*	*Alternaria alternata*
	Mycelia Growth Inhibition (%)	
Gumbo limbo extract	60.37	56.32
AgNP	72.63	63.16
ZnNP	71.58	68.42
CuNP	66.11	65.21

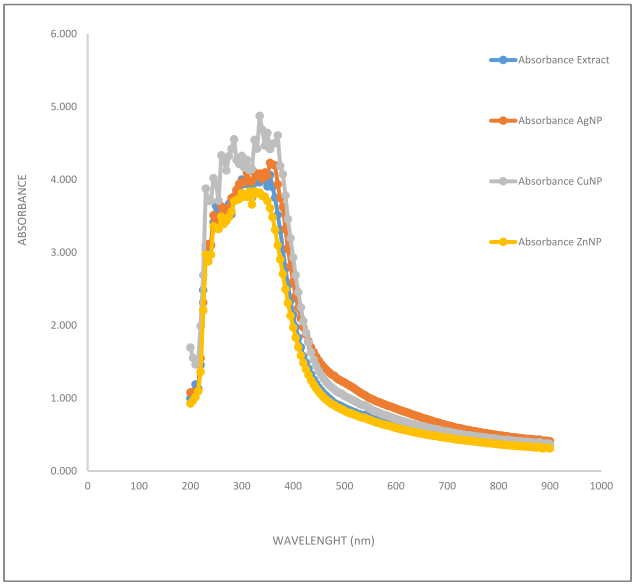

Figure 1: The UV-Visible Characterization (Wavelength scanning) of Bursera simaruba aqueous extract with metallic nanoparticles (AgNP, CuNP, ZnNP)

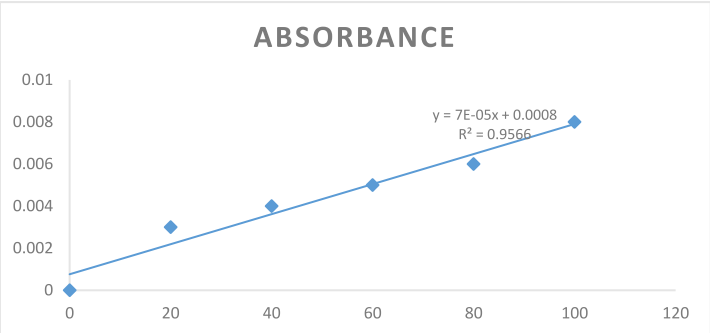

Figure 2: Flavonoid Concentration and Absorbance Graph

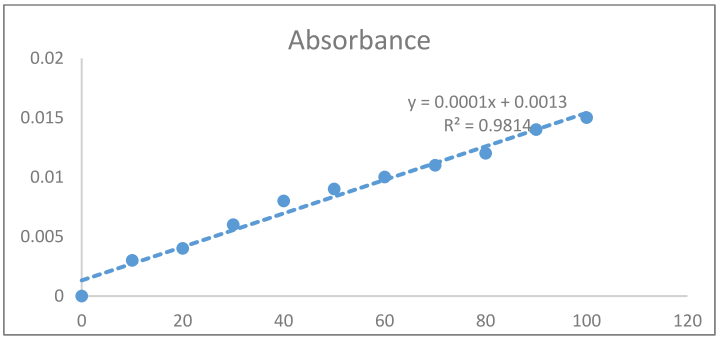

Figure 3: Phenol Concentration and Absorbance Graph

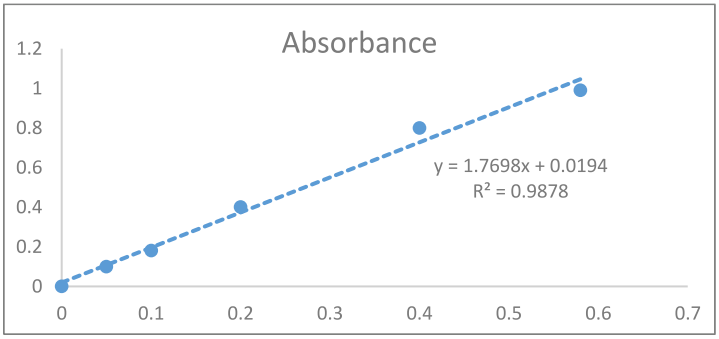

Figure 4: Ascorbic Acid Concentration and Absorbance Graph

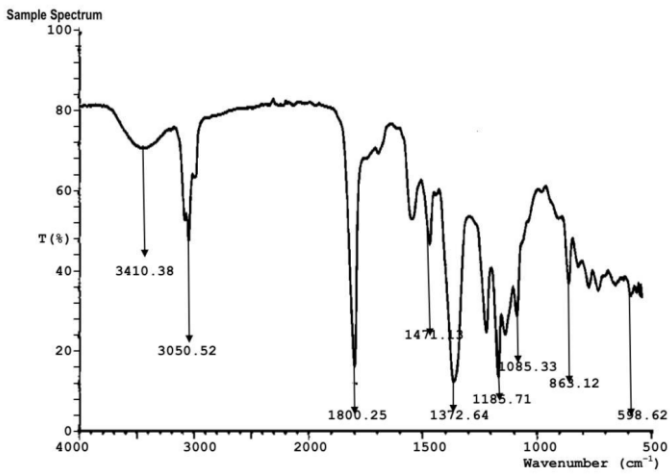

Figure 5: FTIR Analysis of Bursera simaruba Aqueous Extract

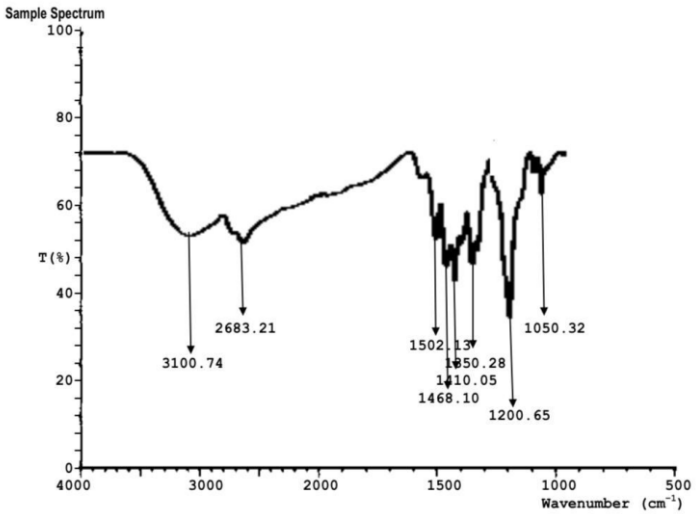

Figure 6: FTIR Analysis of AgNP Nanoparticle

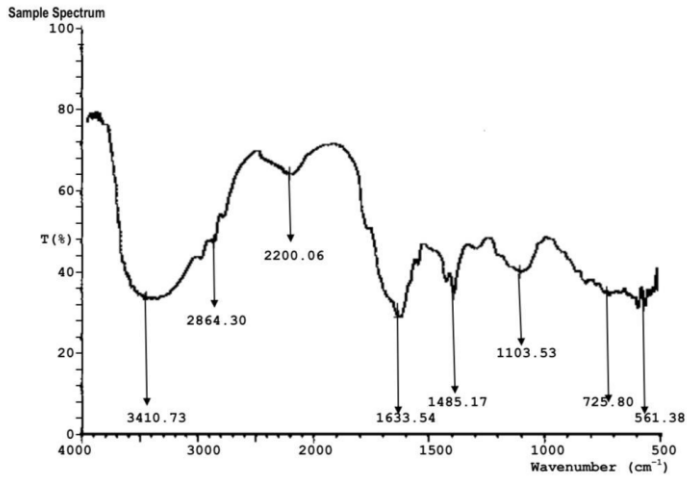

Figure 7: FTIR Analysis of ZnONP

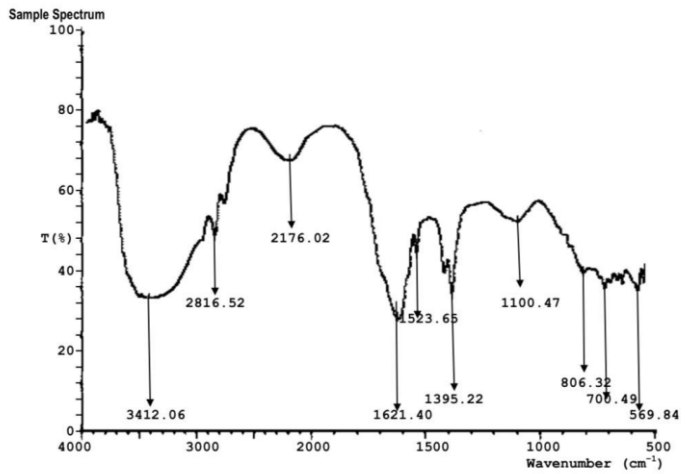

Figure 8: FTIR Analysis of CUNP

Table 9: Ligand Preparation
Identification of Major Phytochemical Constituents of plumeria rubra

S/N	NAME OF LIGAND	CID NO	CANNONICAL SMILES
1.	Ethanamine, N-ethyl-N-nitroso-	5921	CCN(CC)N=O
2.	1,2-Benzenediol	289	C1=CC=C(C(=C1)O)O
3.	Benzaldehyde, 3-hydroxy-	101	C1=CC(=CC(=C1)O)C=O
4.	5-Hydroxymethyl furfural	237332	C1=C(OC(=C1)C=O)CO
5.	4H-Pyran-4-one, 2,3-dihydro-3,5-dihydroxy-6-methyl-	119838	CC1=C(C(=O)C(CO1)O)O
6.	Myrcene	31253	CC(=CCCC(=C)C=C)C
7.	n-Hexadecanoic acid (palmitic acid)	985	CCCCCCCCCCCCCCCC(=O)O
8.	1-Tetradecanol	8209	CCCCCCCCCCCCCCO
9.	Phytol	5280435	C[C@@H](CCC[C@@H](C)CCC/C(=C/CO)/C)CCCC(C)C
10.	4-Dimethylamino-3,5-dinitrobenzoic acid	521460	CN(C)C1=C(C=C(C=C1[N+](=O)[O-])C(=O)O)[N+](=O)[O-]
11.	9,12-Octadecadienoic acid (Z,Z) (linoleic acid)	171042521	CCCCC/C=C/C/C=C/CCCCCCC[13C](=O)O
12.	Benzenepropanoic acid, 3,5-bis(1,1-dimethylethyl)-4-hydroxy-, methyl ester	62603	CC(C)(C)C1=CC(=CC(=C1O)C(C)(C)C)CCC(=O)OC
13.	Hexadecanoic acid, ethyl ester (ethyl palmitate)	11066542	CCCCCC(CCCCCCCCCC(=O)OCC)O
14.	Octadecane, 1-methoxy-	118710610	CC1(CC[C@@H]([C@]23[C@@H]1[C@@H]([C@@]([C@]45[C@H]2CC[C@H]([C@H]4OC(=O)CCCC(=O)N[C@@H](CC6=CC=C(C=C6)N(CCCl)CCCl)C(=O)OC)C(=C)C5=O)(OC3)O)O)O)C
15.	Oleic acid	445639	CCCCCCCC/C=C\CCCCCCCC(=O)O
16.	9,12-Octadecadienoic acid (Z,Z)	6438497	CCCCC/C=C\C(/C=C\CCCCCCCC(=O)O)O
17.	Squalene	638072	CC(=CCC/C(=C/CC/C(=C/CC/C=C(/CC/C=C(/CCC=C(C)C)\C)\C)/C)/C)C
18.	Cyclooctasiloxane, hexadecamethyl-	11170	C[Si]1(O[Si](O[Si](O[Si](O[Si](O[Si](O[Si](O1)(C)C)(C)C)(C)C)(C)C)(C)C)(C)C)(C)C)C

Table 10: Predicted ADME of main phytochemicals of Bursera simaruba

Molecule	Formula	MW	MR	TPSA	iLOGP	ESOL Solubility (mg/ml)	ESOL Class	GI absorption	BBB permeant	Pgp substrate	CYPs Inhibition	Bioavailability Score	log Kp (cm/s)
Ethanamine, N-ethyl-N-nitroso-	$C_4H_{10}N_2O$	102.14	28.98	32.67	1.99	ESOL Solubility (mg/ml)	Very soluble	High	Yes	No	NONE	0.55	-6.58
1,2-Benzenediol	$C_6H_6O_2$	110.11	30.49	40.46	1.13	2.70E+01	Very soluble	High	Yes	No	CYP3A4	0.55	-6.35
Benzaldehyde, 3-hydroxy-	$C_7H_6O_2$	122.12	33.85	37.3	1.02	2.57E+00	Very soluble	High	Yes	No	NONE	0.55	-6.13
5-Hydroxymethylfurfural	$C_6H_6O_3$	126.11	30.22	50.44	0.91	1.78E+00	Very soluble	High	No	No	NONE	0.55	-7.48
4H-Pyran-4-one, 2,3-dihydro-3,5-dihydroxy-6-methyl-	$C_6H_8O_4$	144.13	32.39	66.76	1.19	3.67E+01	Very soluble	High	No	No	NONE	0.85	-7.44
Myrcene	$C_{10}H_{16}$	136.23	48.76	0	2.89	4.55E+01	Soluble	Low	Yes	No	NONE	0.55	-4.17
n-Hexadecanoic acid (palmitic acid)	$C_{16}H_{32}O_2$	256.42	80.8	37.3	3.85	1.22E-01	Moderately soluble	High	Yes	No	CYP1A2, CYP2C9	0.85	-2.77
1-Tetradecanol	$C_{14}H_{30}O$	214.39	70.57	20.23	3.9	2.43E-03	Moderately soluble	High	Yes	No	CYP1A2	0.55	-3.33
Phytol	$C_{20}H_{40}O$	296.53	98.94	20.23	4.85	1.43E-02	Moderately soluble	Low	No	Yes	CYP2C9	0.55	-2.29
4-Dimethylamino-3,5-dinitrobenzoic acid	$C_9H_9N_3O_6$	255.18	65.25	132.18	0.81	3.10E-04	Soluble	High	No	No	NONE	0.56	-6.44
9,12-Octadecadienoic acid (Z,Z) (linoleic acid)	$C_{18}H_{32}O_2$	281.44	89.46	37.3	4.14	5.52E-01	Moderately soluble	High	Yes	No	CYP1A2, CYP2C9	0.85	-3.06
Benzenepropanoic acid, 3,5-bis(1,1-dimethylethyl)-4-hydroxy-, methyl ester	$C_{18}H_{32}O_2$	281.44	89.46	37.3	4.14	2.46E-03	Moderately soluble	High	Yes	No	CYP1A2, CYP2C9	0.85	-3.06
Hexadecanoic acid, ethyl ester (ethyl palmitate)	$C_{18}H_{36}O_3$	300.48	91.09	46.53	4.58	2.46E-03	Moderately soluble	High	Yes	No	CYP1A2	0.55	-3.89
Octadecane, 1-methoxy-	$C_{39}H_{52}Cl_2N_2O_{10}$	779.74	197.97	171.93	0	1.16E-02	Moderately soluble	Low	No	Yes	CYP3A4	0.17	-8.64
Oleic acid	$C_{18}H_{34}O_2$	282.46	89.94	37.3	4.01	1.28E-03	Moderately soluble	High	No	No	CYP1A2, CYP2C9	0.85	-2.6
9,12-Octadecadienoic acid (Z,Z)	$C_{18}H_{32}O_3$	296.44	90.63	57.53	4.01	1.09E-03	Moderately soluble	High	No	No	CYP1A2, CYP2C9	0.85	-2.6
Squalene	$C_{30}H_{50}$	410.72	143.48	0	4.01	1.09E-03	Moderately soluble	High	No	No	CYP1A2, CYP2C9	0.85	-2.6
Cyclooctasiloxane, hexadecamethyl-	$C_{16}H_{48}O_8Si_8$	593.23	148.54	73.84	5.85	1.09E-03	Poorly soluble	High	No	No	NONE	0.55	-4.2

Table 11: Molecular Docking Scores and Key Interactions of Selected Bursera simaruba Phytochemicals with Dipeptidyl Peptidase-4 (DPP4)

Ligand	Binding Affinity
Squalene	-6.2
Phytol	-4.9
Oleic acid	-5.2
n-Hexadecanoic_acid_(palmitic_acid)	-5.1
Myrcene	-4.6
Ethanamine_N-ethyl-N-nitroso-	-4.3
Benzenepropanoic_acid_35-bis(11-dimethylethyl)-4-hydroxy-_methyl_ester	-6.4
Benzaldehyde_3-hydroxy-	-5.4
9,12-Octadecadienoic_acid_(ZZ)	-5.2
9,12-Octadecadienoic_acid_(ZZ)_(linoleic_acid)	-4.6
5-Hydroxymethylfurfural	-5.4
4H-Pyran-4-one_23-dihydro-35-dihydroxy-6-methyl-	-5.3
4-Dimethylamino-35-dinitrobenzoic_acid	-6.8
1-Tetradecanol	-4.3
12-Benzenediol	-4.9

Table 12: Predicted Target of Bursera simaruba Phytochemicals

Phytochemical	Target Key	Target Name	Description	P-Value	MaxTC
1,2-Benzenediol	CAH5B_HUMAN	CA5B	Carbonic anhydrase 5B, mitochondrial	2.407×10^{-8}	1
	MYOC_HUMAN	MYOC	Myocilin	3.332×10^{-25}	0.31
	KAT8_HUMAN	KAT8	Histone acetyltransferase KAT8	6.482×10^{-25}	0.4
Benzaldehyde, 3-hydroxy-	DHB1_HUMAN	HSD17B1	Estradiol 17-beta-dehydrogenase 1	2.693×10^{-42}	0.42
	DHB2_HUMAN	HSD17B2	Estradiol 17-beta-dehydrogenase 2	2.096×10^{-39}	0.42
Myrcene	ERG1_HUMAN	SQLE	Squalene monooxygenase	7.838×10^{-37}	0.39
Squalene	ERG1_HUMAN	SQLE	Squalene monooxygenase	6.108×10^{-80}	0.74
	LSS_HUMAN	LSS	Lanosterol synthase	3.45×10^{-23}	0.47
Oleic acid	FABPH_HUMAN	FABP3	Fatty acid-binding protein, heart	1.196×10^{-26}	1
	LPAR4_HUMAN	LPAR4	Lysophosphatidic acid receptor 4	1.157×10^{-80}	0.44

TARGET GENE NETWORK ANALYSES

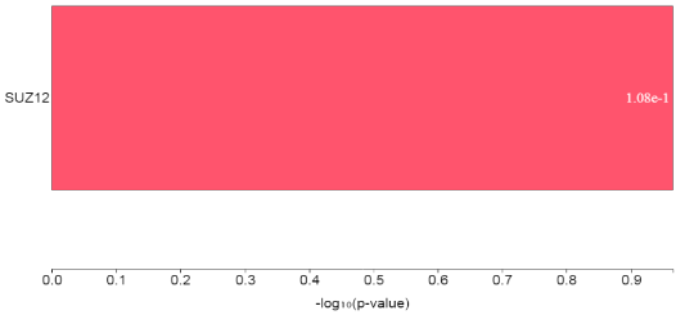

Figure 9a: Transcription factor enrichment analysis (TFEA)

Figure 9b: Protein-Protein Interaction Expansion

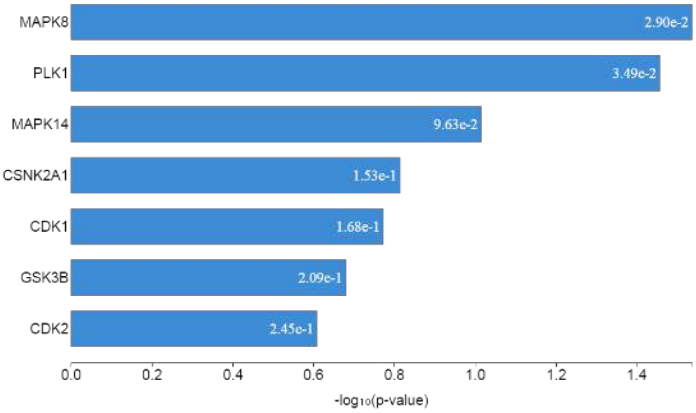

Figure 9c: Kinase enrichment analysis (KEA)

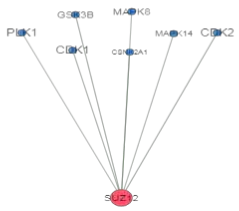

Figure 9d: eXpression2Kinases Network

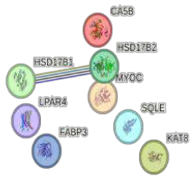

Figure 10: Protein- Protein Interaction of Bursera simaruba Molecular Target

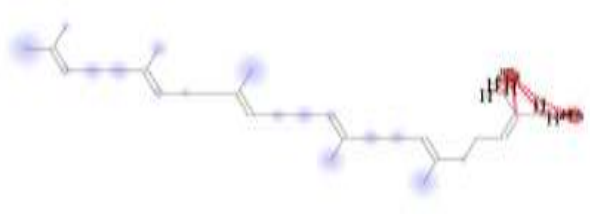

Figure 10a: 2D Representation Showing the Binding of Squalene

Figure 10b: 2D Representation Showing the Binding of Phytol

Figure 10c: 2D Representation Showing the Binding of Oleic Acid

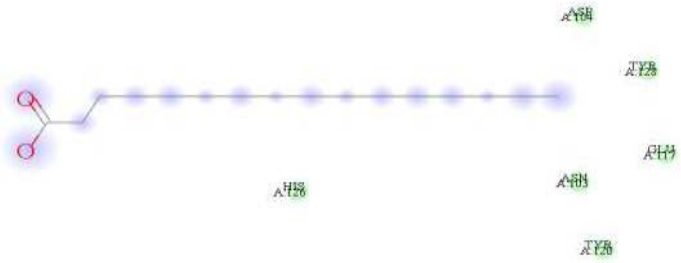

Figure 10d: 2D Representation Showing the Binding of N-Hexadecanoic Acid (Palmitic Acid)

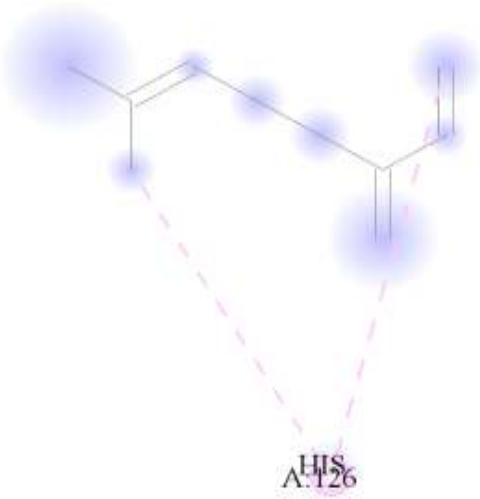

Figure 10e: 2D Representation Showing the Binding of Myrcene

Discussion

Bursera simaruba (commonly known as gumbo limbo) has long been recognized in traditional medicine for treating inflammatory and metabolic conditions. Despite its widespread use, there is still a gap in comprehensive scientific studies that combine phytochemical characterization, eco-friendly nanoparticle synthesis, antimicrobial assessment, and computational prediction of molecular targets. In this study, we examined the proximate and phytochemical constituents of *Bursera simaruba* leaves, assessed their antioxidant and antimicrobial activities, characterized metallic nanoparticles synthesized through green methods, and explored potential therapeutic targets using molecular docking and in silico approaches.

The proximate composition showed that carbohydrates (33.65%) constituted the highest fraction of the leaf, followed by crude protein (17.11%), ash (17.07%), crude fat (15.08%), crude fibre (10.82%), and low moisture content (6.27%). The relatively low moisture level enhances shelf stability and reduces susceptibility to microbial spoilage, supporting its suitability for pharmaceutical preparation. The high ash value reflects a considerable mineral reservoir, corroborating the mineral profile observed in this study.

Comparable studies on medicinal plants have reported similar macronutrient distributions. For instance, nutritional profiling of tropical medicinal leaves demonstrated carbohydrate ranges of 30–45% and protein values between 12–20%, supporting the classification of *B. simaruba* as nutritionally valuable [14]. The relatively high crude fat content observed in this study is consistent with the detection of key fatty acids, including oleic acid, linoleic acid, and palmitic acid. These fatty acids are well recognized for their roles in modulating inflammatory responses and supporting metabolic regulation [15].

The levels of oxalate (1.61 mg/100 g), phytate (13.14 mg/100 g), and tannin (4.14 mg/100 g) were found to be low to moderate, remaining within acceptable dietary thresholds. Although phytates and tannins may reduce mineral bioavailability, they also exert antioxidant and antimicrobial effects through metal chelation and free radical scavenging. Recent evidence indicates that moderate phytate intake is associated with protective cardiovascular and anticancer effects due to its antioxidant activity [16].

The trypsin inhibitor activity (42%) suggests the presence of protease inhibitory compounds. While high levels may reduce protein digestibility, plant-derived protease inhibitors have been increasingly recognized for their anticancer and anti-inflammatory potential [17]. Therefore, within a pharmacological context, these compounds may contribute positively to bioactivity.

The mineral profile demonstrated the presence of potassium, calcium, magnesium, sodium, iron, copper, manganese, and chromium, with minimal lead contamination. Potassium dominance supports electrolyte balance and cardiovascular regulation, while calcium and magnesium contribute to neuromuscular function and metabolic homeostasis.

Trace elements such as iron and copper play central roles in antioxidant enzyme systems, including catalase and superoxide dismutase. The detection of chromium, known to influence insulin sensitivity, further supports the plant's potential relevance in metabolic disorders. Similar mineral compositions have been reported in other medicinal plants used for glycemic control [18].

Qualitative screening revealed abundant saponins and detectable phenols and alkaloids. Quantitatively, flavonoid content (82.86 mg AAE/g) and phenolic content (57.00 mg GAE/g) were high, accompanied by measurable vitamin C (1.97 mg/g). The strong antioxidant performance observed in DPPH (57%), nitric oxide (75%), FRAP (66%), and H_2O_2 (40%) assays confirms the extract's robust redox-modulating capacity.

Phenolics and flavonoids are widely reported as major contributors to antioxidant activity in medicinal plants [19,20]. The strong nitric oxide scavenging effect observed in this study is particularly relevant, as excessive NO production is implicated in inflammatory and metabolic diseases. Comparable antioxidant capacities have been reported for other *Bursera* species, which were attributed to high polyphenolic content [21].

The successful synthesis of AgNPs, ZnONPs, and CuNPs was confirmed by characteristic UV-Visible surface plasmon resonance peaks and FTIR-identified functional groups (–OH, –C=O, –NH). These findings demonstrate that phenolics and flavonoids served as reducing and capping agents.

Green synthesis using plant extracts is widely recognized for producing stable, biocompatible nanoparticles with enhanced antimicrobial properties [12]. The FTIR peaks observed in this study align with previously reported functional groups involved in metal ion reduction during phytogenic nanoparticle synthesis.

The crude extract exhibited mild antibacterial activity, whereas nanoparticle formulations significantly enhanced inhibition zones. AgNPs showed strong activity against *Staphylococcus aureus* and *Klebsiella pneumoniae*, while CuNPs demonstrated superior inhibition against *Streptococcus mutans* and *Salmonella typhi*. Similarly, ZnNPs and AgNPs showed enhanced antifungal activity against *Microphomina phaseolina* and *Alternaria alternata*. These findings are consistent with reports that silver and copper nanoparticles disrupt microbial membranes, generate reactive oxygen species, and interfere with intracellular proteins [22]. The enhanced antimicrobial efficacy compared to crude extract suggests synergistic interactions between metal ions and phytochemicals.

The ADME analysis demonstrated favourable pharmacokinetic profiles for several phytochemicals, including high gastrointestinal absorption and acceptable bioavailability scores (0.55–0.85). Compounds such as 1,2-benzenediol and benzaldehyde derivatives were predicted to be highly soluble and BBB-permeant, suggesting central nervous system accessibility.

Lipophilic compounds such as squalene and fatty acids exhibited moderate solubility but acceptable permeability, consistent with the Lipinski rule of five for drug-likeness [23]. Docking analysis against DPP4 revealed strong binding affinities for 4-dimethylamino-3,5-dinitrobenzoic acid (−6.8 kcal/mol), benzenepropanoic acid derivative (−6.4 kcal/mol), and squalene (−6.2 kcal/mol). These values are within ranges reported for natural DPP4 inhibitors.Fatty acids such as oleic acid and palmitic acid demonstrated stable hydrophobic interactions within the DPP4 active site, consistent with previous reports indicating that long-chain fatty acids can modulate enzymatic targets via hydrophobic binding [22].
Target prediction analysis revealed interactions with CA5B, HSD17B1/2, SQLE, FABP3, LPAR4, and LSS, implicating pathways involved in glucose metabolism, steroid regulation, lipid biosynthesis, and signal transduction. Network analyses (TFEA, KEA, PPI expansion) further indicated multi-target activity, consistent with polypharmacology principles in phytomedicine [24].

Conclusion

Bursera simaruba demonstrates significant antioxidant, antimicrobial, and nanoparticle-mediated bioactivities. Molecular docking and target prediction support its potential antidiabetic mechanism through DPP4 inhibition and metabolic pathway modulation. These findings provide mechanistic insight into its traditional medicinal use and justify further pharmacological and clinical investigations.

REFERENCES

1. World Health Organization. (2023). *WHO traditional medicine strategy: 2014–2023* (Global strategy). https://www.who.int/publications/i/item/9789241506096
2. Li, Q., Li, M., Li, F., Zhou, W., Dang, Y., Zhang, L., & Ji, G. (2020). Qiang-Gan formula extract improves non-alcoholic steatohepatitis via regulating bile acid metabolism and gut microbiota in mice. *Journal of Ethnopharmacology*, *258*, 112896. https://doi.org/10.1016/j.jep.2020.112896
3. Kavalli, K., Hebbar, G. S., Shubha, J. P., Adil, S. F., Khan, M., Hatshan, M. R., Almutairi, A. M., & Shaik, B. (2022). Green Synthesized ZnO Nanoparticles as Biodiesel Blends and Their Effect on the Performance and Emission of Greenhouse Gases. *Molecules*, *27*(9). https://doi.org/10.3390/molecules27092845
4. Liu, Q., Gao, K., Ding, X., Mo, D., Guo, H., Chen, B., Xia, B., Ye, C., Chen, G., & Guo, C. (2023). NAMPT inhibition relieves intestinal inflammation by regulating macrophage activation in experimental necrotizing enterocolitis. *Biomedicine & Pharmacotherapy*, *165*, 115012. https://doi.org/10.1016/j.biopha.2023.115012
5. Martinez, M. A. (2022). Efficacy of repurposed antiviral drugs: Lessons from COVID-19. *Drug Discovery Today*, *27*(7), 1954-1960. https://doi.org/10.1016/j.drudis.2022.02.012
6. Ogbuagu, E. O., Ogbuagu, U., Unekwe, P. C., Nweke, I. N., & Airaodion, A. I. (2020). Qualitative determination of the phytochemical composition of ethanolic extract of *Xylopia aethiopica* fruit. *Asian Journal of Medical Principles and Clinical Practice, 3*(2), 159–166.
7. Airaodion, A. I., Ibrahim, A. H., Ogbuagu, U., Ogbuagu, E. O., Awosanya, O. O., Akinmolayan, J. D., Njoku, O. C., Obajimi, O. O., Adeniji, A. R., & Adekale, O. A. (2019). Evaluation of phytochemical content and antioxidant potential of *Ocimum gratissimum* and *Telfairia occidentalis* leaves. *Asian Journal of Research in Medical and Pharmaceutical Sciences, 7*, 1–11.
8. Airaodion, A. I., Olatoyinbo, P. O., Ogbuagu, U., Ogbuagu, E. O., Akinmolayan, J. D., Adekale, O. A., Awosanya, O. O., Agunbiade, A. P., Oloruntoba, A. P., & Obajimi, O. O. (2019). Comparative assessment of phytochemical content and antioxidant potential of *Azadirachta indica* and *Parquetina nigrescens* leaves. *Asian Plant Research Journal, 2*, 1–14.
9. Airaodion, A. I., & Onabanjo, K. S. (2022). Effect of fortifying zobo (*Hibiscus sabdariffa*) with pineapple and watermelon on the mineral compositions and microbial quality. *Merit Research Journal of Food Science and Technology, 7*(1), 1–7.
10. Esonu, C. E., Iheme, C. I., Njoku, O. C., Agwu, L. O., Edom, C. V., Godian, C. I., Ezerioha, C. C., Airaodion, A. I., & Ujowundu, C. (2024). Investigation of proximate composition and bioactive components in banana (*Musa acuminata*) peels using advanced analytical techniques. *Journal of Nutrition and Food Processing, 7*(10). https://doi.org/10.31579/2637-8914/256
11. Airaodion, A. I., Airaodion, E. O., Ewa, O., Ogbuagu, E. O., & Ogbuagu, U. (2019). Nutritional and anti-nutritional evaluation of garri processed by traditional and instant mechanical methods. *Asian Food Science Journal, 9*(4), 1–13. https://doi.org/10.9734/afsj/2019/v9i430021
12. Adewumi, F. A., Lateef, M. O., Oseni, M. O., Airaodion, A. I., & Oseni, O. A. (2026). Integrated evaluation of *Bauhinia purpurea* leaf: Antimicrobial efficacy and antioxidant potential of leaf extracts and green synthesized silver nanoparticles. *International Journal of Integrative and Complementary Medicine, 2*(1), 1–12. https://doi.org/10.61148/IJICM/013
13. Adewumi, F. A., Ipinlaye, J. O., Owoyemi, A. C., Alonge, F. B., Airaodion, A. I., & Oluyege, A. O. (2026). Distribution, antibiotic sensitivity and biofilm formation of nosocomial pathogens isolated in male and female surgical ward environments from a tertiary hospital in Ado-Ekiti, Ekiti State. *Journal of Clinical Infectious Diseases and Reports, 2*(1), 1–8. https://doi.org/10.59657/jcidr.brs.26.007
14. Esonu, C. E., Iheme, C. I., Njoku, O. C., Agwu, L. O., Dike, C. S., Ohalete, R. O., Mba, B. A., Airaodion, A. I., & Nwaogu, L. A. (2024). Assessment of proximate and biomass composition of cori fibre for potential industrial application. *Journal of Nutrition and Food Processing, 7*(9). https://doi.org/10.31579/2637-8914/255
15. McKee, D. L., Sternberg, A., Stange, U., Laufer, S., & Naujokat, C. (2020). Candidate drugs against SARS-CoV-2 and COVID-19. *Pharmacological Research*, *157*, 104859. https://doi.org/10.1016/j.phrs.2020.104859
16. Pujol, A., Sanchis, P., Grases, F., & Masmiquel, L. (2023). Phytate Intake, Health and Disease: "Let Thy Food Be Thy Medicine and Medicine Be Thy Food". Antioxidants, 12(1), 146. https://doi.org/10.3390/antiox12010146
17. Liu, W., Chen, X., Li, H., Zhang, J., An, J., & Liu, X. (2022). Anti-Inflammatory Function of Plant-Derived Bioactive Peptides: A Review. Foods, 11(15), 2361. https://doi.org/10.3390/foods11152361

18. Uche, C. L., Ugwu, N. I., Ogbenna, A. A., Okite, U. P., Chikezie, K., Ezirim, E. O., Oladele, F. C., Abali, I. O., Nwobodo, M. U., Ejikem, P. I., Otuka, O. A. I., Jibiro, P., Esonu, C. E., & Airaodion, A. I. (2024). Abnormal Haematological Profile caused by Potassium Bromate in Wistar Rats is corrected by Parkia biglobosa seed. *Nigerian journal of physiological sciences : official publication of the Physiological Society of Nigeria*, *39*(1), 119–124. https://doi.org/10.54548/njps.v39i1.15
19. Abali, I. O., Nwobodo, M. U., Uche, C. L., Otuka, O. A. I., Chikezie, K., Omole, O. R., Ezirim, E. O., & Airaodion, A. I. (2023). Protective and curative potential of ethanol leaf extract of *Corchorus olitorius* against potassium bromate-induced renal toxicity. *Asian Journal of Biochemistry, Genetics and Molecular Biology, 13*, 37–46.
20. Iwuoha, C. E., Ezirim, E. O., Onyeaghala, C. A., Orji, S. F., Ugwu, C. N., Igwenyi, C., Uche, C. L., Abali, I. O., Onyekachi, O. I. N., & Nwobodo, M. U. (2022). Perturbation of sex hormones by potassium bromate and preventive effect of African locust bean (*Parkia biglobosa*) seed. *Asian Journal of Research in Biochemistry, 11*, 22–29.
21. Torres-Moreno, H., López-Romero, J. C., Vidal-Gutiérrez, M., Rodríguez-Martínez, K. L., Robles Zepeda, R. E., Vilegas, W., & Oros-Morales, A. (2025). Biological Activities and Phenolic Profile of Bursera microphylla A. Gray: Study of the Magdalena Ecotype. Plants, 14(21), 3357. https://doi.org/10.3390/plants14213357
22. Adewumi, F. A., Oseni, M. O., Madu, V. O., Airaodion, A. I., Akinleye, G.-M. M., Ekundayo, O. A., & Oseni, O. A. (2026). Therapeutic potential of sand box and *in-vitro* biochemical and antimicrobial potentials, metallic nanoparticle, and molecular docking-based screening of key phytochemicals. *International Journal of Biomedical and Clinical Research, 6*(3), 1–14. https://doi.org/10.59657/2997-6103.brs.26.120.
23. Miebs, G., Mielniczuk, A., Kadziński, M., & Bachorz, R. A. (2024). Beyond the Arbitrariness of Drug-Likeness Rules: Rough Set Theory and Decision Rules in the Service of Drug Design. Applied Sciences, 14(21), 9966. https://doi.org/10.3390/app14219966
24. Hopkins, A. (2008). Network pharmacology: the next paradigm in drug discovery. *Nat Chem Biol* **4**, 682–690. https://doi.org/10.1038/nchembio.118